Synthesis, Characterization and Biological Activity of Some Transition Metals Complexes with Schiff Base Derived from 4-Amino-5-phenyl-4*H*-1,2,4-triazole-3-thiol and *p*-Methoxysalicyldehyde

Farag M.A. Altalbawy*, Gehad G. Mohamed† and Mohamed I.A. Mohamed†
National Institute of Laser Enhanced Sciences, Cairo University, Giza-12613, Egypt
E-mail: f_altalbawy@yahoo.com

The coordination behaviour of Schiff base with NOS donation sites, derived from condensation of 4-amino-5-phenyl-4*H*-1,2,4-triazole-3-thiol and *p*-methoxysalicyldehyde (H_2L), transition metal ions namely Cr(III), Mn(II), Co(II) (Cl, ClO_4), Ni(II) (Cl, ClO_4), Cu(II) and Zn(II) are reported. The metal complexes are characterized based on elemental analyses, IR, ^{1}H NMR, solid reflectance, magnetic moment, molar conductance and thermal analyses (TG, DTG and DTA). The ionization constants of the Schiff base under investigation as well as the stability constants of its metal chelates are calculated pH metrically at 25 ºC and ionic strength $\mu = 0.1$ M in 50 % (v/v) ethanol-water mixture. The chelates are found to have trigonal bipyramidal [Co(II), Ni(II), Zn(II)], tetrahedral [Cr(III) and Mn(II)] and square planar [Cu(II)] geometrical structures. The ligand and its binary chelates are subjected to thermal analyses and the different activation thermodynamic parameters are calculated from their corresponding DTG curves to throw more light on the nature of changes accompanying the thermal decomposition process of these compounds. The synthesized ligands, in comparison to their metal complexes also were screened for their antibacterial activity against bacterial species (*Escherichia coli* and *B. subtilis*) and Fungi (*A. niger*, *A. flavus*, *C. albicans* and *C. tropicalis*). The activity data show that the metal complexes have antibacterial and antifungal activity more than the parent Schiff base ligand against one or more bacterial species.

Key Words: 1,2,4-Triazole-3-thiol Schiff base, Metal complexes, Stability constants, Spectroscopy, Molar conductance, Thermal analyses, Biological activity.

INTRODUCTION

Schiff base metal complexes offer an area of increasing interest. These complexes have numerous applications, such as, in the treatment of cancer[1], as anti-bactericide agents[2], as antivirus agents[3], as fungicide agents[4] and for other biological properties[5]. Polynuclear metal complexes are currently attracting considerable interests, much of them arising from their interesting magnetic behaviours such as the single-

†Department of Chemistry, Faculty of Science, Cairo University, Giza-12613, Egypt.

molecule magnet (SMM) properties[6] and their use as precursors of molecule-based magnetic materials[7-10]. Also, polynuclear transition metal complexes containing nitrogen and phenolic oxygen donor atoms are of considerable interest in inorganic and bioinorganic chemistry[11-13]. In our previous studies, metal complexes of polydentate ligands have been synthesized and fully characterized[14-21]. The most motivating features of these ligands are the possibility of using them to synthesize complexes with different modes of bonding having an interesting biological activity.

On the basis of stated facts, the present work is extension to our work and is devoted to the synthesis of new polydentate Schiff base, H_2L, ligand by the conden- sation of *p*-methoxysalicyldehyde with 4-amino-5-phenyl-4*H*-1,2,4-triazole-3-thiol in the molar ratio 1:1 (salicyldehyde derivatives: amine). The reactions of the Schiff base ligands with Cr(III), Mn(II), Co(II) (X = Cl, ClO_4), Ni(II) (X = Cl, ClO_4), Cu(II) and Zn(II) ions, in molar ratio (1:1; ligand:metal ion) were studied. These reactions afforded mono nuclear complexes with different modes of bonding. The structures of the ligand and its metal complexes were characterized by elemental and thermal analyses, IR, ^1H NMR, electronic, as well as conductivity and magnetic susceptibility measurements at room temperature. The biological activities are also studied against some bacterial and fungi organisms.

EXPERIMENTAL

All chemicals used were of the analytical reagent grade (AR) and of highest purity available. They included methyl benzoate (LOBA Chemie), hydrazine hydrate (LOBA Chemie), carbon disulphide (Aldrich) and diethyl ether (Sigma). $CuCl_2 \cdot 2H_2O$ (Sigma); $CoCl_2 \cdot 6H_2O$ and $NiCl_2 \cdot 6H_2O$ (BDH); $ZnCl_2 \cdot 2H_2O$ (Ubichem), $CrCl_3 \cdot 6H_2O$ (Sigma) and $MnCl_2$, $Co(ClO_4)_2 \cdot 6H_2O$ and $Ni(ClO_4)_2 \cdot 6H_2O$ (Sigma) were used. Organic solvents used included absolute ethyl alcohol, diethyl ether and dimethyl formamide. These solvents were spectroscopic pure from BDH. Hydrogen peroxide, sodium chloride, sodium carbonate and sodium hydroxide (AR), hydrochloric acid and nitric acid (Merck) were used. De-ionized water collected from all glass equipments was usually used in all preparations.

Solutions: Fresh stock solution of 1×10^{-3} M ligand; H_2L, was prepared by dissolving the accurately weighed amount of 0.326 g/L in the appropriate volume of absolute ethanol. 1×10^{-3} M Stock solutions of the metal salts ($CrCl_3 \cdot 6H_2O$, 0.266 g/L; $MnCl_2$, 0.125 g/L; $CoCl_2 \cdot 6H_2O$, 0.237 g/L; $Co(ClO_4)_2 \cdot 6H_2O$, 0.366 g/L $NiCl_2 \cdot 6H_2O$, 0.237 g/L; $Ni(ClO_4)_2 \cdot 6H_2O$, 0.366 g/L; $CuCl_2 \cdot 2H_2O$, 0.170 g/L and $ZnCl_2$, 0.136 g/L)) were prepared by dissolving the accurately weighed amounts of the metal salts in the appropriate volume of de-ionized water. The metal salt solutions were standardized by the recommended procedures[22]. Dilute solutions of the metal ions and Schiff base under study were prepared by accurate dilution. For potentiometric studies, all solutions of metal ions were prepared by dissolving the calculated amount of their salts in the least amount of water; then, ethanol was added to the appropriate

volume. 1 M sodium chloride solution was used to keep the ionic strength constant. 0.1 N sodium hydroxide and hydrochloric acid solutions were prepared and standardized by the recommended method[22].

The spectrophotometric measurements in solution were carried out using automated spectrophotometer UV-vis Perkin-Elmer Model Lambda 20 ranged from 200-900 nm. pH measurements were carried out using 716 DMS Titrino Metrohm connected with 728 Metrohm Stirrer. The molar conductance of solid complexes in DMF was measured using Sybron-Barnstead conductometer (meter PM.6, E = 3406). Elemental microanalyses of the separated solid chelates for C, H, N and S were performed at the Microanalytical Center, Cairo University. Infrared spectra were recorded on a Perkin-Elmer FT-IR type 1650 spectrophotometer in 4000-200 cm^{-1} region. The spectra were recorded as KBr pellets. The solid reflectance spectra were measured on a Shimadzu 3101PC spectrophotometer. The molar magnetic susceptibility was measured on powdered samples using the Faraday method. The diamagnetic corrections were made by Pascals constant and Hg[Co(SCN)$_4$] was used as a calibrant. Thermal analyses (TG, DTG and DTA) were carried out in dynamic nitrogen atmosphere (20 mL min^{-1}) with a heating rate of 10 °C min^{-1} using Shimadzu TG-60H and DTA-60H thermal analyzers. The mass spectra were recorded by the EI technique at 70 eV using MS-5988 GS-MS Hewlett-Packard instrument at the Microanalytical Center, Cairo University. The ^{1}H NMR spectra were recorded using 300 MHz Varian-Oxford Mercury at the Microanalytical Center, Cairo University.

Procedures

Potentiometric measurements: Three mixtures were prepared and potentio-metrically titrated at 25 ºC and ionic strength μ = 0.1 (1 M NaCl solution) in purifid nitrogen atmosphere using a digital pH meter (Orion research model 701 A Digital Ionalizer). The pH meter was calibrated before each titration using standard buffer solutions. The n$_A$ (average number of protons associated with the ligand), n (average number of ligand attached per metal ion) and pL (free ligand exponent) values were calculated using a method described by Irving and Rossotti[23].

Synthesis of benzoic hydrazide: It was prepared according to the previously published method[24]. The yield of benzoic hydrazide was found to be 5.8 g (85 %) m.p. 112 ºC (lit. m.p. 112 ºC)[24].

Synthesis of potassium 3-benzoyl dithiocarbazate: It was prepared according to the previously published method[24]. The yield was found to be 20 g (80 %)[24].

Synthesis of 4-amino-5-phenyl-4H-1,2,4-triazole-3-thiol: It was prepared according to the previously published method[25]. The yield was 17 g (85 %) and m.p. 203-204 ºC (lit. m.p. 203-206 ºC)[25].

Synthesis of H$_2$L Schiff base: Hot solution (60 °C) of 4-amino-5-phenyl-4H-1,2,4-triazole-3-thiol (1.92 g, 10 mmol) was mixed with hot solution (60 °C) of p-methoxysalicyldehyde (1.52 g, 10 mmol) in 50 mL ethanol. The resulting mixture was left under reflux for 2 h and the formed solid product was separated by filtration,

purified by crystallization from ethanol, washed with diethyl ether and dried in a vacuum over anhydrous calcium chloride. The yellow product is produced in 83 % yield.

Synthesis of metal complexes: The metal complexes were prepared by the addition of hot solution (60 °C) of the appropriate metal chloride or perchlorate (1 mmol) in an ethanol-water mixture (1:1, 25 mL) to the hot solution (60 °C) of the Schiff base (0.326 g, 1 mmol) in the same solvent (25 mL). The resulting mixture was stirred under reflux for one hour whereupon the complexes precipitated. They were collected by filtration, washed with an ethanol-water mixture (1:1) and diethyl ether. The analytical data for C, H, N and S were repeated twice.

Biological activity: A 0.5 mL spore suspension (10^{-6}-10^{-7} spore/mL) of each of the investigated organisms was added to a sterile agar medium just before solidification, then poured into sterile petri dishes (9 cm in diameter) and left to solidify. Using sterile cork borer (6 mm in diameter), three holes (wells) were made in each dish; then, 0.1 mL of the tested compounds dissolved in DMF (100 g/mL) were poured into these holes. Finally, the dishes were incubated at 37 ºC for 48 h where clear or inhibition zones were detected around each hole. 0.1 mL DMF alone was used as a control under the same condition for each organism and by subtracting the diameter of inhibition zone resulting with DMF from that obtained in each case, both antibacterial activities can be calculated as a mean of three replicates[26].

RESULTS AND DISCUSSION

The required Schiff base namely 2-[(3-mercapto-5-phenyl-4*H*-1,2,4-triazol-4-yl)imino]methyl}-6-methoxyphenol (H$_2$L) have not been reported *hitherto*. It is prepared in this work as depicted in **Scheme-I** and described in the experimental part, crystallized and dried under vacuum and subjected to elemental analyses, mass spectra, IR and ^{1}H NMR.
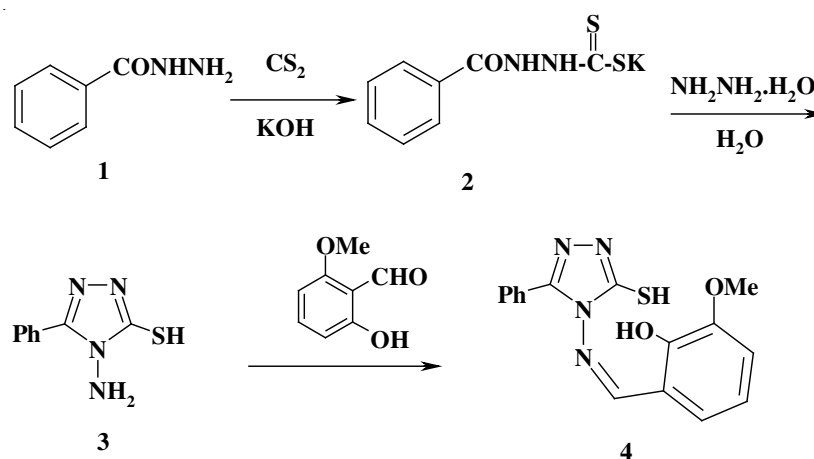
Scheme-I

The results of elemental analyses (C, H, N, S) with molecular formula and the melting point are presented in Table-1. The results obtained are in good agreement with those calculated for the suggested formula and the melting point is sharp indicating the purity of the prepared Schiff base.
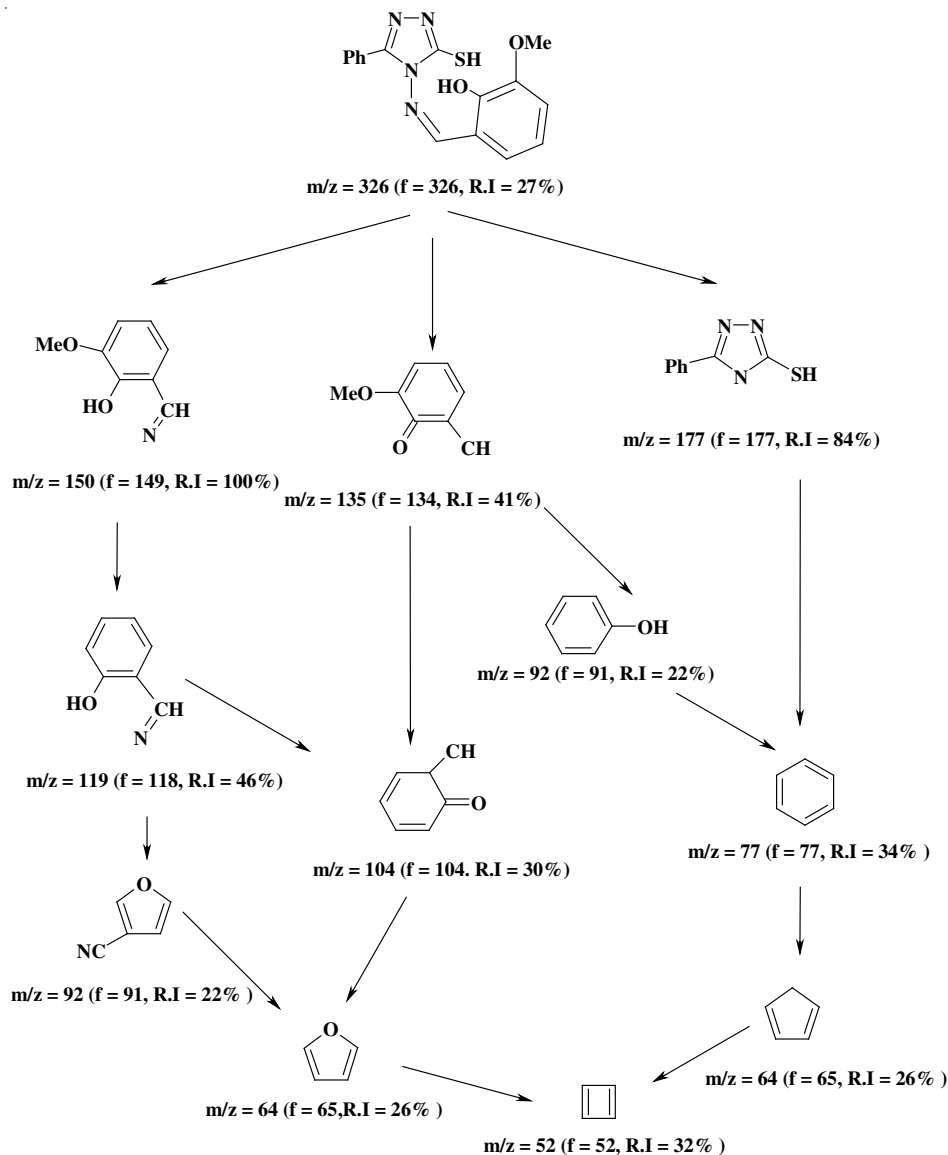
TABLE-1
ANALYTICAL AND PHYSICAL DATA OF H_2L AND ITS METAL COMPLEXES

| Compound | Colour (yield %) | m.p. (°C) | Found (calcd.) (%) | | | | | $\mu_{eff.}$ (BM) | Λ_m Ω^{-1} mol^{-1} cm^2 |
			C	H	N	S	M		
H_2L $C_{16}H_{14}N_4O_2S$	Yellowish	190 ± 2	58.61 (58.89)	4.43 (4.29)	17.39 (17.17)	10.03 (9.81)	–	–	–
$[Cr(HL)(H_2O)]Cl_2 \cdot 3H_2O$ $C_{16}H_{21}N_4O_6SCl_2Cr$	Green (78)	> 300	36.65 (36.92)	4.12 (4.04)	10.89 (10.77)	6.38 (6.15)	10.11 (10.00)	4.53	168
$[Mn(HL)(H_2O)]Cl \cdot 2H_2O$ $C_{16}H_{19}N_4O_5SClMn$	Brown (72)	> 300	36.65 (36.92)	3.92 (4.04)	11.65 (11.92)	6.72 (6.81)	12.01 (11.71)	4.92	79
$[Co(HL)(H_2O)_2]Cl \cdot 2H_2O$ $C_{16}H_{21}N_4O_6SCl_2Co$	Green (78)	> 300	40.54 (40.89)	58.61 (58.89)	4.43 (4.29)	17.39 (17.17)	11.66 (12.00)	5.15	83
$[Co(HL)(H_2O)_2]ClO_4 \cdot 2H_2O$ $C_{16}H_{21}N_4O_{10}SClCo$	Brown (80)	> 300	34.72 (34.56)	39.42 (39.06)	4.49 (4.27)	11.72 (11.39)	10.11 (10.62)	5.09	90
$[Ni(HL)(H_2O)_2]Cl \cdot 2H_2O$ $C_{16}H_{21}N_4O_6SClNi$	Green (80)	> 300	39.59 (39.06)	34.72 (34.56)	3.88 (3.78)	10.41 (10.08)	12.22 (12.03)	3.40	95
$[Ni(HL)(H_2O)_2]ClO_4 \cdot 2H_2O$ $C_{16}H_{21}N_4O_{10}SClNi$	Green (82)	> 300	34.89 (34.56)	39.59 (39.06)	4.50 (4.27)	11.46 (11.39)	10.64 (10.62)	3.33	84
$[Cu(HL)(H_2O)]Cl \cdot H_2O$ $C_{16}H_{17}N_4O_4SClCu$	Green (76)	>300	41.57 (41.74)	34.89 (34.56)	3.64 (3.78)	9.89 (10.08)	13.71 (13.80)	1.96	75
$[Zn(HL)(H_2O)_2]Cl \cdot 2H_2O$ $C_{16}H_{21}N_4O_6SClZn$	Yellow (72)	>300	38.20 (38.55)	4.02 (4.22)	11.32 (11.24)	6.80 (6.43)	12.70 (13.15)	Diam.	81

The structure of the Schiff base is also confirmed by IR and ^1H NMR spectra. The electron impact mass spectrum of H_2L ligand was recorded and investigated at 70 eV of electron energy and the mass fragmentation and the molecular ion peaks of the different suggested fragments of H_2L are shown in **Scheme-II**. It is shown that H_2L gives a well-defined parent peaks at m/z = 326 (RI = 27 %).

The absorption spectrum for 2.5×10^{-3} M solution of H_2L ligand in absolute ethanol at λ ranging from 200-700 nm, against the same solvent as a blank, is carried out. The absorption spectrum of H_2L ligand shows sharp bands at 222 (ε = 2.30×10^3 L mol^{-1} cm^{-1}), 255 (ε = 1.78×10^3 L mol^{-1} cm^2), 290 (ε = 9.60×10^2 L mol^{-1} cm^{-1}) and shoulder band at 330 nm (ε = 3.90×10^2 L mol^{-1} cm^{-1}). These bands can be attributed to π-π*and n-π* transitions within the Schiff bases molecules.

Ligands dissociation and metal-ligand stability constants: The ligands dissociation constant was calculated by the method of interpolation at half $\bar{n}A$ values. It is found that H_2L ligand is found to have a pK_a value of 10.19, which can be attributed to the ionization of the phenolic OH group. The free energy change, $\Delta G°$, was also calculated and found to be -56.30. The negative value indicate the spontaneous character of dissociation reaction.

m/z = 326 (f = 326, R.I = 27%)

m/z = 150 (f = 149, R.I = 100%)

m/z = 135 (f = 134, R.I = 41%)

m/z = 177 (f = 177, R.I = 84%)

m/z = 92 (f = 91, R.I = 22%)

m/z = 119 (f = 118, R.I = 46%)

m/z = 104 (f = 104. R.I = 30%)

m/z = 77 (f = 77, R.I = 34%)

m/z = 92 (f = 91, R.I = 22%)

m/z = 64 (f = 65, R.I = 26%)

m/z = 64 (f = 65,R.I = 26%)

m/z = 52 (f = 52, R.I = 32%)

Scheme-II: Mass fragmentation pattern of H_2L

The stability constants of the Mn(II), Co(II) (X = Cl, ClO$_4$), Cu(II) and Zn(II) complexes with H_2L ligand are determined potentiometriclly using the method described by Irving and Rossotti[23]. The mean log β_1 and log β_2 values are listed in Table-2. Three methods are applied for computing successive stability constants namely Interpolation at half values, correction-term and mid-point. The complex-forming abilities of the transition metal ions are frequently characterized by stability orders. The order of stability constants is found to be $Co^{2+} < Ni^{2+} < Cu^{2+} > Zn^{2+}$ in

accordance with the Irving and Williams order[27] for divalent metal ions of the $3d$ series. It is clear from Table-2 that the stability of Cu(II) complexes are considerably larger as compared to other metals of the $3d$ series. Under the influence of the ligand field, Cu(II) ($3d^9$) will receive some extra stabilization[28] due to tetragonal distortion of octahedral symmetry in their complexes. The Cu(II) complexes will be further stabilized due to the Jahn-Tellar effect[29]. The free energy of formation, ΔG^o, accompanying the complexation reaction has been determined at 25 ºC (Table-2). From the table, it is apparent that the negative values of ΔG^o show that the driving tendency of the complexation reaction is from left to right and the reaction proceeds spontaneously.

TABLE-2
$\log \beta_1$ AND $\log \beta_2$ VALUES FOR METAL COMPLEXES

Ion	Log β_1				Log β_2				$-\Delta G^o$
	(A)	(B)	(C)	(M)	(A)	(B)	(C)	(M)	(kJ mol^{-1})
Mn(II)	5.72	5.53	5.06	5.43	10.26	10.94	10.12	10.44	-51.24
Co(II) (X = Cl)	5.70	5.48	5.02	5.40	10.15	10.81	10.04	10.33	-51.02
Co(II) (X = ClO$_4$)	5.73	5.60	5.09	5.47	10.12	10.74	9.90	10.25	-51.00
Cu(II)	5.89	5.74	5.15	5.59	10.38	11.04	10.18	10.53	-51.62
Zn(II)	5.71	5.51	5.03	5.41	10.18	10.86	10.06	10.36	-51.08

(A) Interpolation at half values method, (B) correction-term method, (C) mid- point method, (M) mean.

Composition and structures of H$_2$L Schiff base complexes: The results of elemental analyses, listed in Table-1 are in good agreement with those required by the proposed formulae. According to the data, the formulae of the complexes are [M(HL)(H$_2$O)$_z$]X·yH$_2$O (M = Mn(II), Co(II), Ni(II), Cu(II) and Zn(II), X = Cl or ClO$_4$, z = 1-2, y = 1-2 and [Cr(HL)(H$_2$O)]Cl$_2$·3H$_2$O.

Molar conductivity measurements: It is concluded from the results listed in Tables-1 that the Cr(III) complex has molar conductivity value of 168 Ω^{-1} mol^{-1} cm^2 indicating its ionic nature and of the type 1:2 electrolyte. On the other hand, the molar conductivity values of Mn(II), Co(II), Ni(II), Cu(II) and Zn(II) chelates are found to be in the range from 75-95 Ω^{-1} mol^{-1} cm^2. It is obvious from these data that these chelates are ionic in nature and they are of the type 1:1 electrolytes.

IR Spectra and mode of bonding: The data of the IR spectra of the Schiff base ligand and its complexes are listed in Table-3. The IR spectra of the complexes are compared with those of the free ligands in order to determine the coordination sites that may involved in chelation. Upon comparison it is found that the ν(C=N) of the azomthine stretching vibration is found in the free ligand at 1580 cm^{-1}. This band is shifted to higher (1586-1582 cm^{-1}) wave numbers in the complexes indicating the participation of the azomethine nitrogen in coordination[17-20]. The ν(OH) and ν(C=O) and δ(OH) stretching vibrations are observed at 3279, 1292 and 1465 cm^{-1}, respectively. The participation of the phenolic O-atom in the

complex formation is evidenced from the disappearance or shift in position of these bands to 3425-3414, 1302-1284 and 1426-1404 cm^{-1} [19]. The SH stretching vibration *i.e.*, $\nu(SH)$, is not of good help since it displayed very weak bands in the free ligand and complexes spectra. However, the participation of the SH group in chelation is ascertained from the shift of the $\nu_{asym}(CS)$ and $\nu_{sym}(CS)$ from 678 and 763 cm^{-1} for the free ligand, respectively, to lower or higher wave numbers in the spectra of the complexes [30].

TABLE-3
KEY IR DATA (cm^{-1}) OF H$_2$L LIGAND AND ITS METAL COMPLEXES

Compound	$\nu(C=N)$	$\nu(SH)$	$\nu(CS)$ (asym.)	$\nu(CS)$ (sym.)	$\nu(OH)$	$\nu(C-O)$	$\delta(OH)$	$\nu(M-N)$	$\nu(M-O)$	$\nu(M-S)$
H$_2$L	1580sh	2340s	678sh	763m	3279sh	1292sh	1465sh	–	–	–
[Cr(HL)(H$_2$O)]Cl$_2$·3H$_2$O	1583sh	2341s	681m	766m	3414br	1289sh	1404sh	509w	558m	460w
[Mn(HL)(H$_2$O)]Cl·2H$_2$O	1583sh	2340s	695sh	770m	3421br	1302sh	1419sh	535s	561m	468w
[Co(HL)(H$_2$O)$_2$]Cl·2H$_2$O	1584sh	2340s	695sh	770m	3423br	1290sh	1422sh	468w	578w	422w
[Co(HL)(H$_2$O)$_2$]ClO$_4$·2H$_2$O	1583sh	2340s	695sh	772m	3422br	1290sh	1423m	495s	580s	437w
[Ni(HL)(H$_2$O)$_2$]Cl·2H$_2$O	1586sh	2339s	696sh	771sh	3421br	1290sh	1425m	464s	580s	428s
[Ni(HL)(H$_2$O)$_2$]ClO$_4$·2H$_2$O	1585sh	2339s	696sh	770m	3423br	1289sh	1425sh	465w	571w	430w
[Cu(HL)(H$_2$O)]Cl·H$_2$O	1582sh	2340s	694m	770m	3425br	1290sh	1426m	453w	576s	422w
[Zn(HL)(H$_2$O)$_2$]Cl·2H$_2$O	1586sh	2340s	696sh	770m	3420br	1284sh	1425sh	529s	585m	468w

sh = sharp, m = medium, br = broad, s = small, w = weak.

The new bands appeared in the complexes at 495-453, 580-571 and 437-422 cm^{-1} are attributed to the $\nu(M-N)$, $\nu(M-O)$ and $\nu(M-S)$, respectively [15]. Therefore, from the IR spectra, it is concluded that H$_2$L ligand behaves as a uninegatively terdentate ligand in all the complexes and coordinated to the metal ions *via* its deprotonated phenolic oxygen beside the azomethine nitrogen and protonated thiophenolic sulphur.

^{1}H NMR spectra: It is found that the phenolic OH, thiol SH, azomethine, Ar-H and -OCH$_3$ signals are found at 14.13 (s, 1H, ArOH), 10.03 (s, 1H, ArSH), 9.40 (s, 1H, azomethine H), 6.93- 7.91 (m, 9H, ArH) and 3.83 ppm (s, 3H, -OCH$_3$) in the spectrum of H$_2$L ligand, respectively. It is found that the phenolic OH signal is disappeared in the spectrum of the Zn(II) complex, indicating its partcipatation in complex formation with proton displacement. The SH signal is also shifted to 9.62 ppm in the spectrum of Zn(II) complex indicating its binding to the metal ions without proton displacement. The azomethine, Ar-H and -OCH$_3$ signals are found in the spectrum of the Zn(II) complex at 9.47 (s, 1H, azomethine H), 6.87-8.01(m, 9H, ArH) and 3.81 ppm (s, 3H, -OCH$_3$), respectively.

Magnetic moment and electronic spectral studies: The single crystal could not be obtained for X-ray analyses to confirm the geometrical structures for these complexes, solid reflectance spectra and magnetic moment measurements are used for this purpose.

The magnetic moment value of the Cr(III) complex (Table-1) is found to be 4.53 B.M. which indicate the presence of Cr(III) complexes in tetrahedral structure[31].

The diffuse reflectance spectrum of the Mn(II) complex shows three bands at 15945, 20765 and 26925 cm^{-1} assignable to $^6A_{1g} \rightarrow {}^4T_{1g}$, $^6A_{1g} \rightarrow {}^4T_{2g}$(G) and $^6A_{1g} \rightarrow {}^4T_{2g}$(D) transitions, respectively[31]. The magnetic moment value is 4.92 B.M. which indicates tetrahedral structure. The electronic spectrum of the Co(II) complex resemble those of other five coordinate Co(II) complexes[14], where three bands are observed at 12900, 16230 and 18550 cm^{-1}. The fourth band at 22955 cm^{-1} refers to the charge transfer band. The low magnetic moment value (μ_{eff} = 5.15 BM) compared with those observed for octahedral or tetrahedral complexes, may support the five coordinate geometry[14].

The solid reflectance spectrum of the Ni(II) complex show recognizable spectral bands at 13990, 18025 and 21850 cm^{-1}. The positions of these spectral bands are quite consistent with those predicted for five coordinate Ni(II) complex whose structure had been established by X-ray crystallographic measurements[32]. The bands can be assigned respectively[31], to $^3B_1 \rightarrow {}^3E$, $^3B_1 \rightarrow {}^3A_2$ and $^3B_1 \rightarrow {}^3E$ transitions assuming the effective symmetry to be C_{4V}. The bands at 27460-28250 cm^{-1} may assign to L $\rightarrow$ MCT band.

The μ_{eff} value of the Cu(II) complex of 1.96 BM indicates a square planar geometry. In confirmation of this structure only one band is seen in the spectra around 14345 cm^{-1} with two shoulders on either sides at 18667 and 11952 cm^{-1}. These are assigned to $^2B_{1g} \rightarrow {}^2A_{1g}$, $^2B_{1g} \rightarrow {}^2B_{2g}$ and $^2B_{1g} \rightarrow {}^2E_{2g}$ transitions, respectively[33]. A moderately intense peak observed at 24850 cm^{-1} is due to ligand to metal charge transfer band.

In analogy with those described for Zn(II) complexes containing N-O donor Schiff bases[34-36] and according to the empirical formulae of these complexes, trigonal bipyramidal geometry is proposed for the Zn(II) complex.

Thermal analyses (TG, DTG and DTA): The TG curve of Schiff base H$_2$L (Fig. 1A), exhibits a first and second estimated mass losses of 67.94 % (calcd. 67.48 %) within the temperature range from 110-340 °C, which may be attributed to the liberation of C$_9$H$_8$N$_4$OS molecule as gases. In the 3rd and 4th stages within the temperature range 340-800 °C, H$_2$L loss the remaining part with an estimated mass loss of 32.56 % (calcd. 32.51 %) with a complete decomposition as CO, CO$_2$, NO, NO$_2$, … *etc.* gases. These mass losses are appeared in the DTA (Table-4) as seven endothermic and seven exothermic peaks within the temperature ranges given.

Table-4 also shows the TG, DTG and DTA results of thermal decomposition of metal chelates. From these results, it is concluded that [Cr(HL)(H$_2$O)]Cl$_2$·3H$_2$O (Fig. 1B) chelate exhibits three decomposition steps. The first step within the temperature range from 30-150 °C (mass loss = 10.53 %; calcd. (%) for 3H$_2$O; 10.38) may accounted for the loss of three water molecules of hydration. The mass losses of the remaining decomposition steps amount to 74.68 % (calcd. 75.00 %). They

TABLE-4
THERMOANALYTICAL RESULTS (TG, DTG AND DTA) OF H_2L AND ITS METAL COMPLEXES

Complex	TG range (°C)	DTG max (°C)	DTA (°C)	n*	Mass loss total mass loss estim (calcd.) %	Assignment	Metallic residue
H_2L	110-171 171-338 338-800	136 230, 260 499	127(-), 138(+), 179(-), 215(+), 236(-), 242(+), 272 (-), 295(+), 323(-), 412(+), 436(-), 448(+), 508(-), 546(+).	1 2 1	5.23 (5.52) 62.71 (61.96) 32.56 (32.51) 100.5 (99.99)	- Loss of H_2O. - Loss of $C_9H_6N_4S$. -Loss of C_7H_6O.	–
[Cr (HL)(H$_2$O)] Cl$_2$·3H$_2$O	30-150 150-297 297-800	135 220 433	122(-), 141(+), 162(-), 179(+), 218(-), 249(+), 275 (-), 450(-), 477(+).	1 1 1	10.53(10.38) 17.97(17.50) 56.70 (57.50) 85.22 (85.38)	- Loss of $3H_2O$. - Loss of 2HCl and H_2O. -Loss of $C_{16}H_{11}N_4O_{1/2}S$.	$0.5Cr_2O_3$
[Co(HL)(H$_2$O)$_2$] Cl·2H$_2$O	30-120 120-325 325-800	58 252 416, 490	58(-), 77(+), 127(-), 181(+), 250(-), 312(+), 442(-), 544(+).	1 1 2	7.53 (7.30) 21.30 (21.05) 56.95 (56.35) 85.70 (84.70)	- Loss of $2H_2O$. - Loss of HCl, $2H_2O$ and OCH_3. -Loss of $C_{15}H_9N_4S$.	CoO
[Ni(HL)(H$_2$O)$_2$] Cl·2H$_2$O	30-130 130-308 308-900	76 270 370, 488	52(-), 82(+), 280(-), 309(+), 371(-), 441(+), 503(-), 524(+).	1 1 2	7.32 (7.30) 20.90 (21.05) 56.25 (56.35) 84.47 (84.70)	- Loss of $2H_2O$. - Loss of HCl, $2H_2O$ and OCH_3. - Loss of $C_{15}H_9N_4S$.	NiO
[Cu (HL)(H$_2$O)] Cl·H$_2$O	30-140 140-382 382-800	86 319 468, 660	52(-), 98(+), 233(-), 268(+), 288(-), 330(+), 352(-), 436(+), 491(-), 539(+), 550(-), 582(+), 631 (-), 750(+).	1 1 2	7.05 (7.32) 21.79 (21.06) 56.34 (56.35) 85.18 (84.73)	- Loss of H_2O. - Loss of H_2O, HCl and OCH_3. - Loss of $C_{15}H_9N_4S$.	CuO
[Zn (HL) (H$_2$O)$_2$]Cl·2H$_2$O	25-140 140-300 300-770	56 247 372, 662	50(-), 76(+), 130(-), 197(+), 267(-), 318(+), 412(+), 445 (-), 595(+), 670(-), 760(+).	1 1 2	7.93 (7.23) 20.08 (20.78) 56.19 (55.62) 84.20 (83.63)	- Loss of $2H_2O$. - Loss of HCl, $2H_2O$ and OCH_3. - Loss of $C_{15}H_9N_4S$.	ZnO

*Number of decomposition steps; (-) = exothermic, (+) = endothermic.

correspond to the removal of 2HCl, H_2O and HL leaving $0.5Cr_2O_3$ as a residue. The DTA data listed in Table-4 shows the exothermic and endothermic peaks accompanying these decomposition steps.
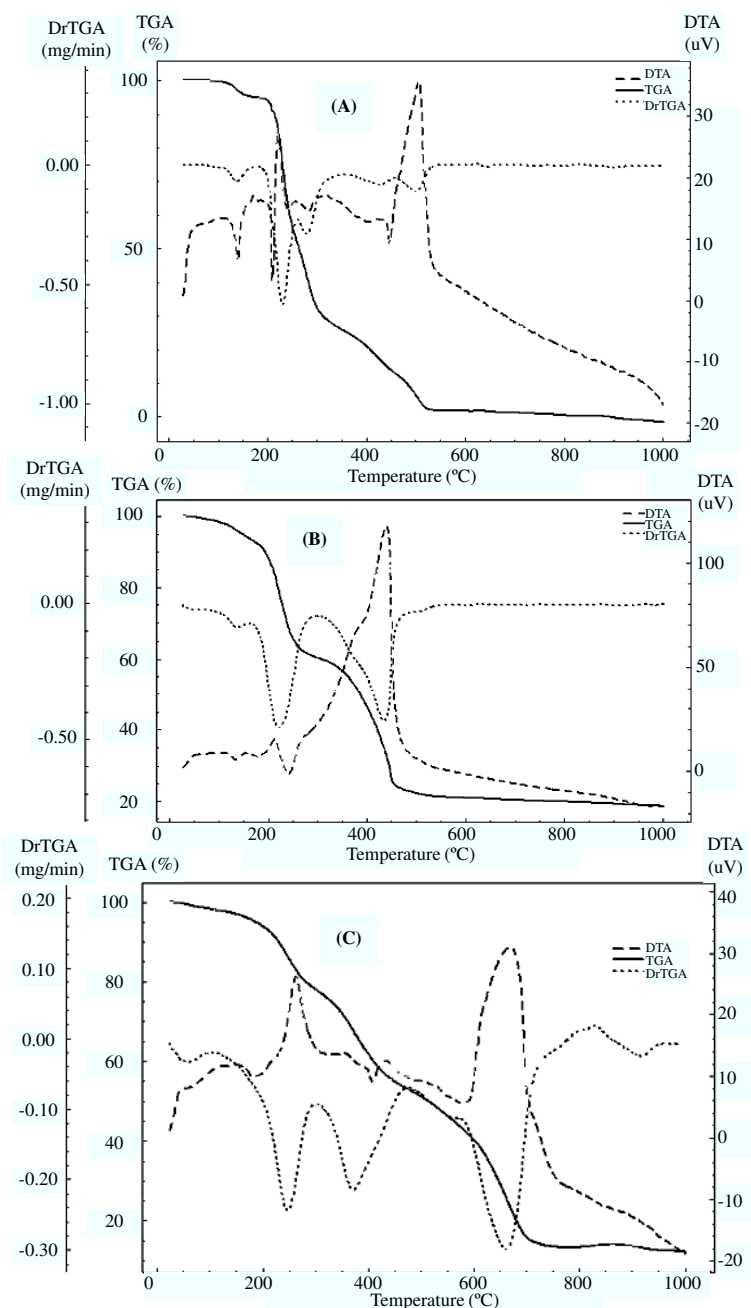

Fig. 1.   Thermal analyses (TG, DTG and DTA) of H_2L and its complexes. Where (A) H_2L ligand, (B) Cr(III) and (C) Zn(II) complexes

The TG, DTG and DTA curve of the Co(II)-HL chelate represents five decomposition steps as illustrated in Table-4. The first step of decomposition within the temperature range from 30-120 °C correspond to the loss of hydrated water molecules with mass loss of 7.05 % [calcd. (%) for $2H_2O$; 7.32]. This mass loss appears in the DTA as exothermic and endothermic peaks within the temperature ranges of decomposition. As shown in Table-4, the mass losses of the remaining decomposition steps amount to 78.13 % [calcd. (%) 77.41]. They correspond to the removal of HCl, $2H_2O$, OCH_3, HL leaving CoO as a residue. The decomposition of this gaseous chelate is appeared in the DTA curve as endothermic and exothermic peaks.

The TG, DTG and DTA curve of the Ni(II)-HL chelate shows four stages of decomposition within the temperature range of 30-900 °C. The first stage at 30-130 °C corresponds to the loss of water molecules of hydration for both complexes. While the subsequent (2nd, 3rd and 4th) stages involve the loss of HCl, $2H_2O$, OCH_3 and ligand molecule, respectively. The overall weight loss amounts to 84.47 % (calcd. 84.67 %). The DTA data listed in Table-4 shows the presence of endothermic and exothermic peaks within the temperature ranges of decomposition.

On the other hand, $[Cu(HL)(H_2O)]Cl \cdot H_2O$ chelate exhibits four decomposition steps. The first step within the temperature range from 30-140 °C [mass loss = 3.93; calcd. (%) for H_2O; 3.91] may accounted for the loss of water molecules of hydration. The mass losses of the remaining decomposition steps amount to 78.87 % (calcd. 78.90 %). They correspond to the removal of HCl, H_2O, OCH_3 and HL leaving CuO as a residue. The DTA data are listed in Table-4.

The TG, DTG and DTA curve of the Zn(II) chelate (Fig. 1C) represents four decomposition steps as illustrated in Table-4. The first step of decomposition within the temperature range 25-140 °C corresponds to the loss of hydrated water molecules with a mass loss of 7.93 % (calcd. For $2H_2O$; 7.24 %). The mass losses of the remaining decomposition steps amount to 76.27 % (calcd. (%) 76.68), within the temperature rang from 140-770 °C. This correspond to the removal of HCl, $2H_2O$, OCH_3, HL leaving ZnO as a residue. The DTA data give exothermic peaks at 50, 130, 267, 445 and 670 °C and endothermic peaks at 76, 197, 318, 412, 595 and 760 °C.

Kinetic data: The thermodynamic activation parameters of decomposition processes of dehydrated complexes namely activation energy (E*), enthalpy (ΔH*), entropy (ΔS*) and Gibbs free energy change of the decomposition (ΔG*) were evaluated graphically by employing the Coats-Redfern relation[36]:

$$\log\left[\frac{\log\{W_f/(W_f-W)\}}{T^2}\right] = \log\left[\frac{AR}{\theta E*}\left(1-\frac{2Rt}{E*}\right)\right] - \frac{E*}{2.303RT} \quad (1)$$

where W_f is the mass loss at the completion of the reaction, W is the mass loss up to temperature T; R is the gas constant, E* is the activation energy in kJ mol^{-1}, θ is the heating rate and $[1-(2RT/E*)] \cong 1$. A plot of the left-hand side of eqn. 1 against 1/T gives a slope from which E* was calculated and A (Arrhenius factor) was

determined from the intercept. The entropy of activation (ΔS^*), enthalpy of activation (ΔH^*) and the the free energy change of activation (ΔG^*) were calculated and the the data obtained are summarized in Table-5. The activation energies of decomposition were found to be in the range 19.35-165.70 and 16.90-329.60 kJ mol^{-1}. The high values of the activation energies reflect the thermal stability of the complexes. The entropy of activation was found to have negative values in all the complexes which indicate that the decomposition reactions proceed with a lower rate than the normal ones.

TABLE-5
THERMODYNAMIC DATA OF THE THERMAL DECOMPOSITION
OF METAL COMPLEXES OF H$_2$L

Complex	Decomp. temp. ($°C$)	E* (kJ mol^{-1})	A (s^{-1})	ΔS^* (kJ mol^{-1})	ΔH^* (kJ mol^{-1})	ΔG^* (kJ mol^{-1})
[Cr(HL)(H$_2$O)]Cl$_2$·3H$_2$O	30-110	27.46	7.20×10^7	-82.19	26.89	32.47
	110-170	58.17	7.95×10^4	-144.8	57.01	77.20
	170-300	62.12	1.04×10^5	-146.4	60.27	92.82
	300-480	134.4	4.36×10^9	-63.44	130.8	158.1
[Co(HL)(H$_2$O)$_2$]Cl·2H$_2$O	30-120	16.90	4.33×10^8	-66.15	16.41	20.33
	130-200	51.08	1.06×10^6	-125.5	49.56	72.48
	200-330	77.14	9.78×10^5	-128.9	75.03	107.8
	330-470	168.2	1.50×10^{12}	-14.15	164.7	170.6
[Ni(HL)(H$_2$O)$_2$]Cl· 2H$_2$O	30-180	96.57	2.57×10^9	-53.72	90.01	13.23
	190-310	76.36	3.02×10^5	-139.3	74.09	112.0
	310-420	120.6	2.54×10^8	-85.88	117.5	149.6
	430-540	329.6	1.94×10^{22}	-177.7	325.5	238.8
[Cu(HL)(H$_2$O)]Cl·H$_2$O	30-140	27.88	8.73×10^7	-82.61	27.16	34.30
	150-290	67.85	1.21×10^5	-146.9	65.57	105.8
	300-380	71.55	1.86×10^5	-144.6	68.90	114.9
	380-510	91.70	2.69×10^5	-144.8	87.80	155.8
[Zn(HL)(H$_2$O)$_2$]Cl·2H$_2$O	30-100	31.81	1.55×10^7	-93.19	31.35	36.47
	100-310	35.58	4.70×10^7	-96.43	33.54	57.19
	310-480	61.20	4.92×10^6	-118.6	58.12	102.1
	480-730	166.4	2.39×10^9	-71.99	160.9	208.4

Structural interpretation: The structures of the complexes of Schiff base with Cr(III), Mn(II), Co(II) (X = Cl, ClO$_4$), Ni(II) (X = Cl, ClO$_4$), Cu(II) and Zn(II) ions shown in Fig. 2.

Biological activity: The main aim of the production and synthesis of any anti-microbial compound is to inhibit the causal microbe without any side effects on the patients. In addition, it is worthy to stress here on the basic idea of applying any chemotherapeutic agent which depends essentially on the specific control of only one biological function and not multiple ones. The chemotherapeutic agent affecting only one function has a highly sounding application in the field of treatment by anticancer, since most anticancers used in the present time affect both cancerous diseased cells and healthy ones which in turns affect the general health of the patients. Therefore, there is a real need for having a chemotherapeutic agent which controls only one function.
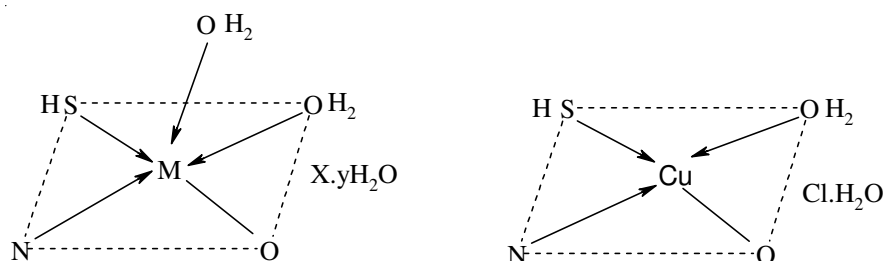
M = Co(II), X = Cl, ClO$_4$, y = 2.
    Ni(II), X = Cl, ClO$_4$, y = 2.

Fig. 2. Structural formulas of H$_2$L metal complexes

In testing the antibacterial and antifungal activity of these compounds, more than one test organism was used to increase the chance of detecting antibiotic principles in tested materials. The sensitivity of a microorganism to antibiotics and other antimicrobial agents was determined by the assay plates which incubated at 28 ºC for two days for yeasts and at 37 ºC for one day for bacteria.

All of the tested compounds showed a remarkable biological activity against different types of gram-positive (*Bacillus subtilis* ATTC 6051), gram-negative bacteria (*Escherichia coli* ATTC 11775) and fungi (*A. niger*, *A. flavus*, *C. albicans* and *S. pyogones*). The data are listed in Table-6. On comparing the biological activity of the Schiff bases and their metal complexes, the following results are obtained: H$_2$L ligand is found to have biological activity against all tested bacteria. But metal complexes are found to have sensitivity for inhibition of gram-positive more than gram-negative bacteria. According to the data listed in Table-6 and Fig. 3, biological activity of metal complexes are found to follow the order Cu(II) > Co(II) (X = Cl) > Ni(II) (X = Cl) > H$_2$L > Ni(II) (X = ClO$_4$) > Co(II) (X = ClO$_4$). Therefore, it is concluded that the presence of metal ions as the result of complexation enhance the biological activity of the parent Schiff base. And also Schiff base H$_2$L ligand shows antifungal activity against *A. niger* and *C. albicans*. From Table-6, H$_2$L is found to have high sensitivity against *A. niger* than *C. albicans*. Metal complexes have antifungal biological activity and follow the order Ni(II) (X = Cl) > Cu(II) > Ni(II) (X = ClO$_4$) > Co(II) (X = ClO$_4$) > Co(II) (X = Cl). It is also clear from Table-6 and Fig. 3 that the metal complexes are found to have more or less antifungal activity more than the parent H$_2$L$_2$ ligand.

Also the data listed in Table-6 show that *E. coli* is inhibited by metal complexes. The importance of this lies in the fact that these complexes could be applied fairly in the treatment of some common diseases caused by *E. coli e.g.*, septicaemia, gastroenteritis, urinary tract infections and hospital aquired infections[37-39].

TABLE-6
BIOLOGICAL ACTIVITY AND MIC$_{50}$ OF H$_2$L LIGAND AND ITS METAL COMPLEXES

Sample	Bacteria		Fungi			
	E. coli	*B. subtilis*	*A. niger*	*A. flavus*	*C. albicans*	*C. tropicalis*
H$_2$L	2.2 >100 µg/mL	2.3 >100 µg/mL	1.0 >100 µg/mL	-ve —	0.9 >100 µg/mL	-ve —
[Cr(HL)(H$_2$O)]Cl$_2$.3H$_2$O	1.4 >100 µg/mL	1.6 >100 µg/mL	-ve —	0.6 >100 µg/mL	0.7 50 µg/mL	-ve —
[Mn(HL)(H$_2$O)]Cl.2H$_2$O	4.0 >100 µg/mL	4.2 >100 µg/mL	0.7 >100 µg/mL	1.3 >100 µg/mL	-ve —	1.6 >100 µg/mL
[Co(HL)(H$_2$O)$_2$]Cl·2H$_2$O	2.7 >100 µg/mL	2.6 >100 µg/mL	0.5 50 µg/mL	0.6 50 µg/mL	-ve —	0.7 50 µg/mL
[Co(HL)(H$_2$O)$_2$]ClO$_4$.2H$_2$O	1.5 >100 µg/mL	1.8 >100 µg/mL	0.9 50 µg/mL	-ve —	0.4 50 µg/mL	-ve —
[Ni(HL)(H$_2$O)$_2$]Cl·2H$_2$O	2.4 >100 µg/mL	2.3 >100 µg/mL	1.8 50 µg/mL	-ve —	0.8 50 µg/mL	-ve —
[Ni(HL)(H$_2$O)$_2$]ClO$_4$·2H$_2$O	2.0 50 µg/mL	2.1 50 µg/mL	-ve —	1.1 50 µg/mL	-ve —	0.8 50 µg/mL
[Cu(HL)(H$_2$O)]Cl·H$_2$O	3.0 12.5 µg/mL	3.2 25 µg/mL	0.8 50 µg/mL	-ve —	1.4 50 µg/mL	-ve —
[Zn(HL)(H$_2$O)$_2$]Cl·2H$_2$O	4.5 >100 µg/mL	5.0 >100 µg/mL	-ve —	0.8 50 µg/mL	0.6 50 µg/mL	-ve —

Test was done using the diffusion agar technique. Inhibition values = 0.1-0.5 cm beyond control = +. Inhibition values = 0.6-1.0 cm beyond control = ++. Inhibition values = 1.1-1.5 cm beyond control = +++.
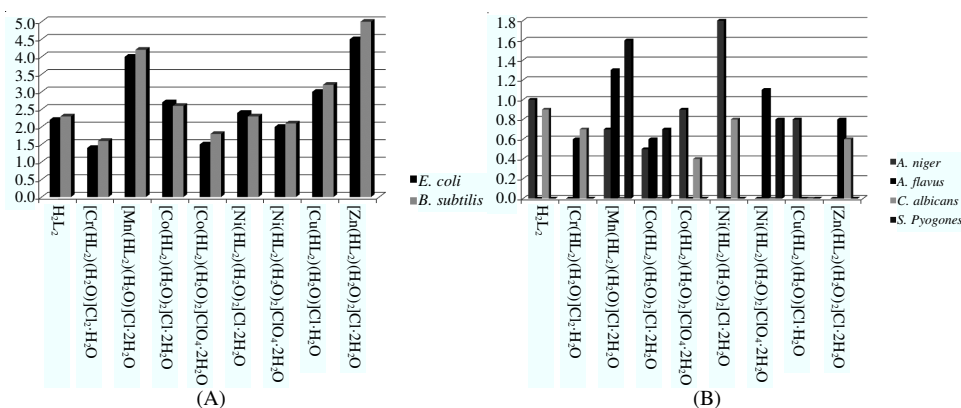

Fig. 3. Bacterial (A) and fungal (B) activity of H$_2$L and its metal complexes

It is believed that all the complexes which are biologically active against both the gram-negative strains may have something to do with the barrier function of the envelope of these gram-negative strains activity, acting in a way similar to that described by Brown[40] and Nikaido *et al.*[41]. Therefore, it is claimed here that the synthesis of these complexes might be recommended and/or established a new line for search to new antitumor particularly when one knows that many workers studied the possible anti tumor action of many synthetic and semi synthetic compounds[42-44].

REFERENCES

1. M. Wang, L.F. Wang, Y.Z. Li, Q.X. Li, Z.D. Xu and D.Q. Ou, *Transition Met. Chem.*, **26**, 307 (2001).
2. N.N. Gulerman, S. Rollas, H. Erdeniz and M. Kiraj, *J. Pharm. Sci.*, **26**, 1 (2001).
3. P. Tarasconi, S. Capacchi, G. Pelosi, M. Corina, R. Albertini, A. Bonati, P.P. Dall'Aglio, P. Lunghi and S. Pinelli, *Bioorg. Med. Chem.*, **8**, 154 (2000).
4. J. Charo, J.A. Lindencrona, L.M. Carlson, J. Hinkula and R. Kiessling, *Virol. J.*, **78**, 11321 (2004).
5. V. Mishra, S.N. Pandeya and S. Anathan, *Acta Pharm. Turc.*, **42**, 139 (2000).
6. D. Gatteschi and R. Sessoli, *Angew. Chem. Int. Ed.*, **42**, 268 (2003).
7. H. Miyasaka, K. Nakata, K. Sugiura, M. Yamashita and R. Clérac, *Angew. Chem. Int. Ed.*, **43**, 707 (2004).
8. R. Clérac, H. Miyasaka, M. Yamashita and C. Coulon, *J. Am. Chem. Soc.*, **124**, 12837 (2002).
9. L. Lecren, O. Roubeau, C. Coulon, Y.G. Li, X.L. Goff, W. Wernsdorfer, H. Miyasaka and R. Clérac, *J. Am. Chem. Soc.*, **127**, 17353 (2005).
10. L. Lecren, W. Wernsdorfer, Y.G. Li, A. Vindigini, H. Miyasaka and R. Clérac, *J. Am. Chem. Soc.*, **129**, 5045 (2007).
11. E.I. Solomon, R.K. Szilagyi, S.D. George and L. Basumallick, *Chem. Rev.*, **104**, 419 (2004).
12. S. Leininger, B. Olenyuk and P.J. Stang, *Chem. Rev.*, **100**, 853 (2000).
13. M. Du, X.J. Zhao, J.H. Guo, X.H. Bu and J. Ribas, *Eur. J. Inorg. Chem.*, 294 (2005).
14. G.G. Mohamed, *Spectrochim. Acta*, **64A**, 188 (2006).
15. G.G. Mohamed, M.M. Omar and A.M.M. Hindy, *Spectrochim. Acta*, **62A**, 1140 (2005).
16. A.A. Soliman and G.G. Mohamed, *Thermochim. Acta*, **421**, 151 (2004).
17. G.G. Mohamed and C.M. Sharaby, *Spectrochim. Acta*, **66A**, 949 (2007).
18. M.M. Omar, G.G. Mohamed and A.A. Ibrahim, *Spectrochim. Acta*, **73A**, 358 (2009).
19. S.M. Abdallah, G.G. Mohamed, M.A. Zayed and M.S.A. El-Ela, *Spectrochim. Acta*, **73A**, 833 (2009).
20. G.G. Mohamed and Z.H. Abd El-Wahab, *J. Therm. Anal. Cal.*, **73**, 347 (2003).
21. G.G. Mohamed, M.M. Omar and A.A. Ibrahim, *Eur. J. Med. Chem.*, **44**, 4801 (2009).
22. A.I. Vogel, Quantitative Inorganic Analysis Including Elemental Instrumental Analysis, Edn. Second, Longmans, London (1962).
23. (a) H. Irving and H.S. Rossotti, *J. Chem. Soc.*, 3397 (1953); (b) H. Irving and H.S. Rossotti, *J. Chem. Soc.*, 2904 (1954).
24. K. Sung and A.R. Lee, *J. Heterocycl. Chem.*, **29**, 1102 (1992).
25. A.S. Shawali, E.S. Darwish and F.M.A. Altalbawy, *Asian J. Spectros.*, **11**, 113 (2008).
26. N. Sari, S. Arslan, E. Logoglu and I. Sakiyan, *J. Sci.*, **16**, 281 (2003).
27. H. Irving and R.J.P. Williiams, *Nature*, **162**, 746 (1948).
28. R.D. Jones, D.A. Summerville and F. Basolo, *Chem. Rev.*, **79**, 139 (1979).
29. L.E. Orgel, An Introduction to Transition Metal Chemistry Ligand Field Theory, Methuen, p. 55 (1966).
30. A.A. Soliman and W. Linert, *Thermochim. Acta*, **333**, 67 (1999).
31. F.A. Cotton, G. Wilkinson, C.A. Murillo and M. Bochmann, Advanced Inorganic Chemistry, edn. 6, Wiley, New York (1999).

32. A.J. Lavery and M. Schroder, *Acta Crytallogr.*, **CS2**, 37 (1996).
33. P.R. Shukla, V.K. Singh, A.M. Jaiswal and G. Narain, *J. Indian Chem. Soc.*, **60**, 321 (1983).
34. G.G. Mohamed, F.A. Nour El-Dien and N.E.A. El-Gamel, *J. Thermal Anal. Cal.*, **67**, 135 (2002).
35. N.E.A. El-Gamel and G.G. Mohamed, *J. Thermal Anal. Cal.*, **81**, 111 (2005).
36. M.M. Omar, G.G. Mohamed and A.M.M. Hindy, *J. Thermal Anal. Cal.*, **86**, 315 (2006).
37. A.W. Coats and J.P. Redfern, *Nature*, **20**, 68 (1964).
38. E. Jawetz, J.L. Melnick and E.A. Adelberg, Review of Medical Microbiology, Lang Medical Publications, Los Anglos, California, edn. 16 (1979).
39. W.H. Hughes and H.C. Stewart, Concise Antibiotic Treatment, Butter Worth, London (1970).
40. N.R.W. Brown, Resistance of Pseudomonas aeruginosa, John Wiley 71 (1975).
41. H. Nikaido and T. Nakae, *Adv. Microbiol. Physiol.*, **20**, 163 (1979).
42. E.M. Hodnett, A.W. Wu and F.A. French, *Eur. J. Med. Chem. Chem. Ther.*, **13**, 577 (1987).
43. J.A. Hickman, *Biochemie*, **60**, 997 (1987).
44. T. Inoue, Y. Yamashita, M. Nishihara, S. Sugiyama, Y. Sonoda, T. Kumabe, M. Yokoyama and T. Tominaga, *Neuro-Oncol*, **11**, 151 (2009).